

NASA TECHNICAL NOTE



NASA TN D-7858

NASA TN D-7858

(NASA-TN-D-7858) = DESIGN, PERFORMANCE, AND
CALCULATED ERROR OF A FARADAY CUP FOR
ABSOLUTE BEAM CURRENT MEASUREMENTS OF
600-MeV PROTONS (NASA) = 39 p HC \$3.75

N75-21093

Unclas

CSSL 20H H1/73 18181



DESIGN, PERFORMANCE, AND CALCULATED ERROR
OF A FARADAY CUP FOR ABSOLUTE BEAM CURRENT
MEASUREMENTS OF 600-MeV PROTONS

Sherwin M. Beck

Langley Research Center

Hampton, Va. 23665



1. Report No. NASA TN D-7858	2. Government Accession No.	3. Recipient's Catalog No.	
4. Title and Subtitle DESIGN, PERFORMANCE, AND CALCULATED ERROR OF A FARADAY CUP FOR ABSOLUTE BEAM CURRENT MEASUREMENTS OF 600-MeV PROTONS		5. Report Date April 1975	6. Performing Organization Code
		8. Performing Organization Report No. L-9933	10. Work Unit No. 506-16-35-01
7. Author(s) Sherwin M. Beck		11. Contract or Grant No.	13. Type of Report and Period Covered Technical Note
9. Performing Organization Name and Address NASA Langley Research Center Hampton, Va. 23665		14. Sponsoring Agency Code	
		12. Sponsoring Agency Name and Address National Aeronautics and Space Administration Washington, D.C. 20546	
15. Supplementary Notes			
16. Abstract <p>A mobile self-contained Faraday cup system for beam current measurements of nominal 600-MeV protons has been designed, constructed, and used at the NASA Space Radiation Effects Laboratory. The cup is of reentrant design with a length of 106.7 cm and an outside diameter of 20.32 cm. The inner diameter is 15.24 cm and the base thickness is 30.48 cm. The primary absorber is commercially available lead hermetically sealed in a 0.32-cm-thick copper jacket.</p> <p>Several possible systematic errors in using the cup are evaluated. The largest source of error arises from high-energy electrons which are ejected from the entrance window and enter the cup. All other errors are at least 1 order of magnitude lower. A total systematic error of -0.83 percent is calculated to be the decrease from the true current value.</p> <p>From data obtained in calibrating helium-filled ion chambers with the Faraday cup, the mean energy required to produce one ion pair in helium is found to be 30.76 ± 0.95 eV for nominal 600-MeV protons. This value agrees well, within experimental error, with reported values of 29.9 eV and 30.2 eV.</p>			
17. Key Words (Suggested by Author(s)) Faraday cup Charge collection Proton-beam measurement		18. Distribution Statement Unclassified - Unlimited New Subject Category 73	
19. Security Classif. (of this report) Unclassified	20. Security Classif. (of this page) Unclassified	21. No. of Pages 38	22. Price* \$3.75

CONTENTS

SUMMARY	1
INTRODUCTION	1
SYMBOLS	2
FARADAY CUP DESIGN AND CONSTRUCTION	2
Cup Design	2
Cup Construction	3
Vacuum System	4
Faraday Cup Carriage	5
Magnet Design and Performance	5
CALCULATED CURRENT MEASUREMENT ERRORS	6
Delta Ray Escape	6
Tertiary Electron Production	7
Compton Electron Production	7
Ion Formation	8
Inelastic Proton-Nucleus Collisions	8
Strain Currents	8
ESTIMATE OF TOTAL ERROR	9
CALIBRATION OF ION CHAMBERS WITH THE FARADAY CUP	9
CONCLUDING REMARKS	10
APPENDIX A – ERROR PRODUCED BY DELTA RAYS	12
APPENDIX B – ERROR PRODUCED BY COMPTON ELECTRONS	15
APPENDIX C – IONIZATION OF RESIDUAL GAS	20
APPENDIX D – CHARGE LOST THROUGH PROTON-NUCLEUS COLLISIONS	21
REFERENCES	27
TABLES	29
FIGURES	31

PRECEDING PAGE BLANK NOT FILMED

DESIGN, PERFORMANCE, AND CALCULATED ERROR OF A
FARADAY CUP FOR ABSOLUTE BEAM CURRENT
MEASUREMENTS OF 600-MeV PROTONS

Sherwin M. Beck
Langley Research Center

SUMMARY

A Faraday cup was designed and constructed for absolute beam current measurements of 600-MeV protons produced in the NASA Space Radiation Effects Laboratory. The movable Faraday cup assembly has an estimated weight of 616.9 kg. The cup alone has an outside diameter of 20.32 cm, an inside diameter of 15.24 cm, a base thickness of 30.48 cm, a total length of 106.7 cm, and a weight of 235.9 kg. It is constructed of natural lead encased in a copper jacket.

Several possible errors associated with incident proton interactions with various parts of the assembly are evaluated. A calculated systematic error of -0.83 percent is obtained as the decrease from the true current value.

From data obtained in calibrating helium-filled ion chambers with the Faraday cup, the mean energy required to produce one ion pair in helium is found to be 30.76 ± 0.95 eV for nominal 600-MeV protons. This value agrees well, within experimental error, with reported values of 29.9 eV and 30.2 eV.

INTRODUCTION

As part of an experimental program to obtain differential cross sections for the production of charged secondary particles from elemental materials under 600-MeV-proton irradiation, a Faraday cup was designed, constructed, and used as an absolute proton beam monitor at the NASA Space Radiation Effects Laboratory (SREL). For maximum utilization in the three main experimental areas of the laboratory, the cup was designed as a mobile self-contained instrument complete with vacuum pumping equipment, vacuum read-out gage, electromagnet, and magnet power supply.

The design of the cup was based on available information in the literature (refs. 1 to 6), experience of SREL staff members, and constraints imposed by requiring a mobile system. The design was also influenced by the availability of materials and the need to complete the cup in a relatively short period of time. In order to produce a mobile cup

with a 100-percent charge collection efficiency, the arbitrary decision was made to design the cup for incident proton beams with circular cross section of 10 cm or less and to make the cup base 15 to 20 percent larger than the range of 600-MeV protons.

This report describes the features of the Faraday cup system and its use as an absolute charge collector. In addition, calculations have been performed to determine the magnitude of several possible sources of error in using the cup.

SYMBOLS

d_t	distance through volume defined by electrodes
dE/dx	rate of energy loss per unit path length in absorber
$N_{d,e}$	number of delta rays per proton produced in Faraday cup base that escape cup
$N_{d,w}$	number of delta rays per proton scattered into Faraday cup from entrance window
W	mean energy required to produce an ion pair in helium
X	distance of lead from point of production of gamma ray to surface of Faraday cup
μ	mass attenuation coefficient
ρ	density of helium

Subscripts:

exp	experimental
th	theoretical

FARADAY CUP DESIGN AND CONSTRUCTION

Cup Design

During the initial planning for the Faraday cup, it became apparent that (1) one cup at a fixed location in SREL could not meet the varied requirements of the laboratory users,

(2) constructing three or more Faraday cups for the various experimental areas of SREL was not practical, and (3) a movable self-contained Faraday cup system would provide the greatest efficiency and utilization. Because no known Faraday cup had been constructed for 600-MeV-proton charge collection, the author and SREL staff members decided arbitrarily to design the base of the cup with a thickness at least 15 percent greater than the range of 600-MeV protons and to have a reentrant cup with the reentrant portion at least four times the inside diameter of the cup. The proposed diameter of the cup, 40.6 cm, would be two times the beam-tube diameter of the beam transport system. The estimated weight of a cup of these dimensions was over 1360 kg including the vacuum system. The large weight and size of the proposed cup would make it too difficult to use or to move from one area to another. Thus, the decision was made to design the cup for use with proton beams of 10-cm diameter or less, since beams of this size were easily obtained at that time.

After a maximum beam diameter was selected, the outer diameter of the cup was made equal to twice the beam diameter or 20.32 cm. The inner diameter of the reentrant portion of the cup was made 15.24 cm to give a wall thickness of 2.54 cm. The length of the reentrant portion was chosen to be five times the inner diameter or 76.2 cm. Since the range of 600-MeV protons is 25.2 cm in copper and 25.99 cm in lead, the depth of the cup base was made approximately 17 percent greater than either range (30.48 cm). The outside diameter and the length of the cup were set at 20.32 cm and 106.7 cm, respectively.

The first choice for the cup material was copper. However, the time and cost required to produce a copper cup were considered excessive. The cup was then designed to have a lead core with a copper jacket. Thus the cup alone weighed 235.9 kg.

After construction of the cup had begun, the decision was made to build an electromagnet to suppress delta rays from the entrance window and electrons back streaming from the cup base. A cylindrical thin-walled (0.32-cm-thick) copper extension was designed to attach to the cup, and the vacuum housing was modified to accommodate the extension. The magnet was designed to produce a 0.1-tesla field across a 15.25-cm air gap. The vacuum housing extension was designed to extend beyond the cup extension so that the cup extension was slightly more than half way across the magnetic volume. This configuration was chosen so that electrons back streaming from the cup would be deflected into the wall of the cup extension and the delta rays from the entrance window would be deflected into the wall of the vacuum housing.

Cup Construction

A schematic diagram of the Faraday cup assembly is shown in figure 1. The shell of the cup was constructed of a copper sheet 0.32 cm thick. The primary absorber was commercially available lead which was poured into the copper shell. All seams in the

jacket were silver soldered to hermetically seal the lead and prevent possible outgassing. The interior of the jacket was thoroughly cleaned prior to the lead fill, and then all exterior surfaces were cleaned to remove dirt and oil acquired during construction and handling.

The three insulating supports for the cup were machined from tetrafluoroethylene rods, 30.48 cm long and 7.62 cm in diameter, and each support had a saddle with a radius of curvature equal to that of the cup. The minimum thickness of each support was 5.08 cm. Each support was thoroughly cleaned and then bolted to the vacuum chamber base plate. (Minimum cup to bolt distance was 5.08 cm.) The cup was then mounted on the insulating supports with the three 1.91-cm-long copper pegs on the cup placed in the predrilled hole in each support. The pegs prevented longitudinal slippage of the cup and the cradle minimized lateral motion.

The estimated weight of the Faraday cup system, 616.9 kg, is given in table I along with the weights of the major components. This estimate does not include such items as bolts, ion gage readout controller, electrical connectors, and support brackets for the magnet. Initially there was some concern that the weight of the cup would deform the supports and cause the cup extension to contact the vacuum chamber. However, after 7 yr of usage, there has been no noticeable change in the supports.

Electrical connection to the cup was made with a bare copper wire, 0.16 cm in diameter, which was bolted to the cup and soldered to a coaxial feed through in the vacuum chamber base plate.

Vacuum System

The vacuum chamber for the Faraday cup was constructed from stainless steel with a 0.00162-mm finish on interior surfaces. All feed throughs were made in the 1.9-cm-thick base plate which was bolted to the upper removable portion of the chamber. An O-ring, 0.35 cm in diameter, was used to hermetically seal the upper chamber to the base plate. The chamber extension was constructed of aluminum and bolted to the chamber. The entrance window to the cup was 0.05-cm-thick aluminum foil.

The pumping system consisted of a 750 liter/sec oil diffusion pump equipped with a liquid-nitrogen cold trap and a 0.00613 m³/sec mechanical pump. The diffusion pump was mounted directly to the chamber base plate and pumped the chamber through a 10.16-cm-diameter hole in the plate. With the diffusion pump hot and 298 K water to cool the pump, the chamber could be pumped from atmospheric pressure to less than 5×10^{-5} torr (1 torr = 133 Pa) in approximately 10 min. After approximately 1 hr the pressure would reach a steady level of 10^{-6} to 2×10^{-6} torr. When liquid nitrogen was used in the cold trap, the chamber pressure could be held at less than 5×10^{-8} torr.

Two major problems related to ionization of the residual gas were discovered and corrected during the initial operation of the cup. In the original design of the Faraday cup assembly, it was decided to use a 120 liter/sec titanium sublimation pump, rather than an oil diffusion pump, to avoid possible problems with the back streaming of oil. However, during the first attempt to use the sublimation pump, large random variations in output current were observed which were quickly traced to the back streaming of ions from the pump. The magnitude of the variations precluded any use of the cup for accurate current measurements. An attempt was made to suppress the ions by installing an insulated wire grid between the pump and vacuum chamber and by applying a voltage to the grid. It was possible to minimize, but not eliminate, the problem. The reduced flow of ions still produced unacceptably large current variations. The titanium sublimation pump was then replaced by a 400 liter/sec oil diffusion pump equipped with a baffle and cold trap.

The second problem was related to the use of an ionization gage to measure the chamber pressure. The location of the ionization gage was directly below the front end of the cup, and the cup intercepted the ions streaming from the gage filament. The 10^{-5} torr range setting of the ionization gage control unit produced a steady 1- μ A current output. With the gage off, random current fluctuations no greater than 0.01 pA were observed.

Faraday Cup Carriage

An open rectangular box frame (101.6 cm high, 45.72 cm wide, and 137.16 cm long) was constructed from 5.08- by 5.08- by 0.32-cm steel angles. All corners were reinforced with 0.32-cm-thick gusset plates welded to the angles. The frame was then welded to two 111.76-cm-long sections of 15.24-cm steel channel. Two 360^o swivel caster assemblies (steel wheels 12.7 cm in diameter) were mounted to each channel section, and leveling jacks were mounted outside the casters on the channels. The base plate of the vacuum chamber was bolted to the frame to increase the strength and rigidity of the frame. Lifting the assembly by using the leveling jacks at opposite corners produced no apparent twisting of the frame.

Positioning of the cup along the beam center line has proved to be relatively simple with the aid of a plum bob and level. After some experience in using the cup, most experimenters could position the cup, attach cooling water lines to the diffusion pump, make the necessary electrical connections, and pump down the vacuum chamber to less than 5×10^{-5} torr in approximately 1 hr.

Magnet Design and Performance

A C-type electromagnet was designed and constructed for use as a delta ray suppressor at the mouth of the cup. The magnet yoke was constructed of SAE 1010 steel, and

the magnet coil was made from B & S 17-gage copper wire wound on a copper spool. A 12.70-cm-diameter shaft was fitted into the spool end, and the arms of the magnet were bolted to the shaft. The pole faces were tapered from 17.78 cm to 13.97 cm in diameter with an air gap of 16.51 cm. Total weight of the magnet was approximately 81.6 kg.

A regulated 1.5-kW dc power supply was the current source. The field at the center of the air gap, as measured with a Hall probe, was 0.11 tesla for a current of 3 A at 170 V dc. Figure 2 shows the cup extension, and figure 3 shows the magnetic field strength along the extension center line for 3-A current in the coil. The reduction in the maximum field strength was attributed to shielding by the 0.64-cm-thick aluminum wall of the vacuum tank extension and parasitic loss in the nearby steel vacuum tank. The shape of the intensity along the center line is related to the magnet face design.

Because the magnet coil was not constructed with cooling capability, the coil temperature and, consequently, the coil resistance limited the duration of magnet operation. With the magnet coil at room temperature and a constant current of 3 A, the voltage of the constant current supply would increase with the increase in coil resistance from approximately 170 V dc to the maximum output of 400 V dc in approximately 30 min. At this point the current would begin decreasing as the coil temperature continued increasing, and the magnetic flux in the cup extension would decrease with the current.

As shown subsequently, the delta rays from the entrance window are estimated to be the largest source of error. Although this error is calculated to be less than 1 percent, an attempt was made to see whether the magnetic field across the cup extension would suppress this source of error. The test involved measuring the current from a helium-filled ion chamber and from the Faraday cup with and without power to the electromagnet. Approximately 25 different beam currents were used for each test. The ratio of ion chamber current to Faraday cup current gave the number of ion pairs per proton for each current setting. The average value and standard deviation of the ratio were 34.93 ± 1.73 ion pairs per proton with 3-A coil current (approximately 0.07 tesla at the center of the cup extension). Without the magnet current the ratio was 36.31 ± 1.08 ion pairs per proton, an increase of 4 percent from the value with the magnet current. Although the difference between the ratios indicates that the magnetic field does suppress the delta rays, the large standard deviations for the ratios indicate that this difference may not be statistically significant. In addition, these data were taken on different days with different helium supplies and, therefore, the difference between ratios may also indicate a systematic error.

CALCULATED CURRENT MEASUREMENT ERRORS

Delta Ray Escape

The charge measured from a Faraday cup is always in error to a degree because of interactions of the incident particle beam with the nuclei and atomic electrons in the

entrance window and in the cup base. These interactions generate both fast and slow electrons which modify the true incident charge. Delta rays (or knock-on electrons) are produced through collisions of the incident particles with atomic electrons. Delta rays produced in the entrance window are predominantly scattered forward, and a fraction of these electrons enters the cup and reduces the true charge. In appendix A the number of delta rays produced in the entrance window and the number produced in the cup base are calculated. Because of the reentrant design of the cup, the number $N_{d,e}$ of delta rays produced in the cup base that can backscatter out of the cup is much less than the number $N_{d,w}$ of delta rays scattered into the cup from the entrance window. The calculated percent decrease from the true proton current is

$$\frac{N_{d,w} - N_{d,e}}{100} = 0.88 \text{ percent}$$

Tertiary Electron Production

Tertiary electrons are low-energy electrons produced in electron-electron collisions. Relativistic electrons from the entrance window and cup base interact with the various parts of the cup assembly to give rise to this additional source of electrons. Since this is a tertiary process, the number of electrons produced is much smaller than the number of delta rays.

Since there was no electrical insulation between the diffusion pump and the vacuum chamber, the chamber and entrance window were grounded through the diffusion pump; in addition, a second ground was used to insure a zero potential on the vacuum chamber. The electrometer used to measure the cup current was of the vibrating reed type and maintained the cup potential at a few microvolts above ground potential. This slight positive potential on the cup not only tended to attract low-energy electrons from around the outside of the cup but also tended to retain the tertiary electrons produced in the cup. The net result was a negligible decrease in the measured current from the true current.

Compton Electron Production

Another source of error in the measured current from the Faraday cup is loss of charge from the outer surface of the cup by electrons ejected from the surface through the Compton effect. To estimate the charge lost by Compton electrons, the following assumptions were made:

- (1) Each incident proton undergoes an inelastic collision and produces one 3-MeV gamma ray.
- (2) The probability of producing a gamma ray at a given distance in the base is a function of the inelastic proton-nucleus cross section.

(3) The gamma rays are emitted isotropically from the point of the inelastic collision.

(4) The probability that a 3-MeV gamma ray will reach the copper jacket on the cup is given by $\exp(-\mu X)$ where μ is the mass attenuation coefficient and X is the distance in g/cm^2 of lead from the point of production to the surface.

A Monte Carlo computer program incorporating these assumptions was written to describe the transport of protons into the cup base, the emission and attenuation of gamma rays, and the production of Compton electrons. The results of the Monte Carlo calculations are given in table II for different incident beam radii, and the details of the calculations are found in appendix B.

Ion Formation

The residual gas in and around the cup is ionized by the incident proton beam and, to a lesser extent, by secondary electrons and gamma rays. If the gas pressure is sufficiently high, the resulting ions can cause fluctuations in the observed current; or if there is a bias on the cup, there may be a net migration of ions to the cup which would bias the current output. As shown in appendix C the number of ion pairs produced per incident proton at the normal operating pressure of 5×10^{-5} torr is negligibly small compared with other possible errors.

Inelastic Proton-Nucleus Collisions

In appendix D the loss of charge due to protons escaping from the cup through various nucleon-nucleon and proton-nucleus interactions is calculated. The most likely mechanism for proton leakage from the cup is neutron-proton collisions near the surface of the cup. In appendix D the details of the calculations are given along with the various assumptions that were made. Table III shows the percent charge lost by escaping protons for incident parallel proton beams with diameters from 0 to 12 cm.

The cross sections for the production of pi-mesons are generally 1 to 2 orders of magnitude below the cross sections for nucleon emission around 600 MeV. Therefore, the expected charge loss from the cup by mesons is negligible compared with charge losses due to neutron-proton interactions.

Strain Currents

Strain currents from the tetrafluoroethylene insulators were found to be less than 0.01 pA which was the lower limit of the electrometer used for the measurements. Generally, the Faraday cup is used for beam current measurements above 1 pA and the strain currents are ignored.

ESTIMATE OF TOTAL ERROR

Table IV summarizes the estimated error from various phenomena associated with the cup. The values indicated are taken for a 12-cm-diameter input beam as the worst case. As shown in the table, the total estimated error was -0.83 percent, and delta rays from the window were the largest source of error. The other errors were an order of magnitude less than the delta ray error.

CALIBRATION OF ION CHAMBERS WITH THE FARADAY CUP

The primary use of the Faraday cup at SREL has been to calibrate ionization chambers and to measure the full intensity of the external proton and alpha-particle beams. In a series of experiments to obtain the differential scattering cross sections for protons of various elemental targets, a helium-filled ion chamber (ref. 7) was calibrated with the Faraday cup and then used as the beam current monitor during the measurements. The ionization chamber was constructed from drawings supplied by the Neutron Physics Division of the Oak Ridge National Laboratory.

The calibration curve for the ion chamber is shown in figure 4. The number of ion pairs per proton is given by the ratio

$$\frac{\text{Ion pairs}}{\text{Proton}} = \frac{\text{Integrated ion chamber current}}{\text{Integrated Faraday cup current}}$$

The instrumentation used to obtain the data was calibrated against a secondary current standard which had a stated worst-case accuracy of ± 1.6 percent from 0.001 nA to 0.01 nA, ± 1.3 percent from 0.01 nA to 0.1 nA, ± 1.1 percent from 0.1 nA to 1 nA, and ± 0.8 percent from 1 nA to 10 nA.

The data of figure 4 gave the number of ion pairs per proton as 36.31 with a standard deviation of 1.08. The chamber was operated at 100 V, and helium flow through the chamber was approximately 236 cm³/sec. The helium used was of standard commercial grade.

The response of the ion chamber to 600-MeV protons can be computed from

$$\left(\frac{\text{Ion pairs}}{\text{Proton}}\right)_{\text{th}} = \frac{(dE/dx)d_t\rho}{W} = 37.05$$

where

$$dE/dx = 2.4436 \frac{\text{MeV-cm}^2}{\text{g-proton}} \text{ (ref. 8)}$$

$$W = 29.9 \frac{\text{eV}}{\text{Ion pair}}$$

$$d_t = 2.54 \text{ cm}$$

$$\rho = 0.17847 \frac{\text{mg}}{\text{cm}^3}$$

The value for W used in the calculation was taken from reference 9 where the number was derived from experiments with 340-MeV protons. No estimate of the uncertainty in the value of W was given. A value of W of 30.2 eV is reported in table 6 on page 233 of reference 10 for polonium alpha particles.

The experimental value

$$\left(\frac{\text{Ion pairs}}{\text{Proton}} \right)_{\text{exp}} = 36.31 \pm 1.08$$

obtained from the data in figure 4 does not include the calculated systematic error of the cup. Using the error bias of -0.83 percent yields a new value of

$$\left(\frac{\text{Ion pairs}}{\text{Proton}} \right)_{\text{exp}} = 36.01 \pm 1.08$$

which agrees with the calculated value within the uncertainty of the measurement. If this value is used to calculate the energy required to produce an ion pair in helium, the result is

$$W_{\text{exp}} = \frac{(dE/dx)d_t\rho}{\left(\frac{\text{Ion pair}}{\text{Proton}} \right)_{\text{exp}}} = 30.76 \pm 0.95 \text{ eV}$$

for nominal 600-MeV protons.

CONCLUDING REMARKS

The utility of a mobile self-contained Faraday cup system for beam current measurements of 600-MeV protons has been demonstrated during the past 7 yr at the NASA Space Radiation Effects Laboratory. The Faraday cup system, which has an estimated

weight of 616.9 kg, is mounted on casters and can be easily moved. Normally one person can set up the system for beam current measurements in approximately 1 hr.

Several possible errors in using the cup for beam current measurements of 600-MeV protons have been evaluated. The calculated systematic error for all sources considered is approximately -0.83 percent. The largest single source of error arises from delta rays entering the cup from proton-electron interactions in the entrance window. For nondiverging, incident proton beams, the errors associated with all other radiation-producing mechanisms in the cup are an order of magnitude less than the delta ray error.

From data obtained in calibrating helium-filled ion chambers with the Faraday cup, the mean energy required to produce one ion pair in helium was found to be 30.76 ± 0.95 eV for nominal 600-MeV protons. This value agrees well, within experimental error, with reported values of 29.9 eV obtained with 340-MeV protons and 30.2 eV obtained with polonium alpha particles.

Langley Research Center,
National Aeronautics and Space Administration,
Hampton, Va., February 5, 1975.

APPENDIX A

ERROR PRODUCED BY DELTA RAYS

To estimate the effect of knock-on electrons from the window, the cross section for proton-electron collisions as given in reference 11 is used. This expression, in the notation of the present paper, is

$$d\sigma = \pi \frac{N_A Z}{A} r_e^2 \frac{2m_e}{\beta^2} \frac{dT'}{(T')^2} \left[1 - \beta^2 \frac{T'}{T'_{\max}} + \frac{1}{2} \left(\frac{T'}{T + m_p} \right)^2 \right] \quad (A1)$$

where

r_e	classical radius of electron, 2.8178 fm
m_e	rest mass of electron, 0.511 MeV
β	speed of incident proton in terms of velocity of light, 0.792
T'	kinetic energy lost by proton in collision
T	kinetic energy of proton before collision
m_p	rest mass of incident proton, 938.256 MeV
T'_{\max}	maximum kinetic energy loss allowed by conservative laws
N_A	Avogadro's number, 6.0225×10^{23} atoms/mol
Z	atomic charge of element, 13 for aluminum
A	mass number of element, 26.98 for aluminum

The energy T' (as a function of θ) attained by an electron in collision with a 600-MeV proton is given by equation 3 on page 14 of reference 11, which, except for notation, is

APPENDIX A

$$T' = 2m_e \frac{p_p^2 \cos^2 \theta}{\left[m_e + \left(p_p^2 + m_p^2 \right)^{1/2} \right]^2 - p_p^2 \cos^2 \theta} \quad (\text{A2})$$

where

p_p momentum of proton, 1218.98 MeV/c at 600 MeV

c velocity of light

θ angle of electron deflection relative to proton incident direction, deg

The maximum energy T'_{\max} is given by equation (A2) for $\theta = 0^\circ$.

As shown in figure 2, the Faraday cup extension has an outside diameter of 13.02 cm and is located 11.69 cm from the entrance window. In use of the cup, the incident proton beam was parallel and had a diameter of less than 2.54 cm. However, if the diameter of the parallel beam is assumed to be 5.08 cm, it is then possible for delta rays in the angular range from $\theta = 0^\circ$ to $\theta = 38.2^\circ$ to enter the cup. The corresponding energy of these electrons would then vary from $T'_{\max} = 1.72$ MeV for $\theta = 0^\circ$ to $T' = 0.67$ MeV for $\theta = 38.2^\circ$ as given by equation (A2).

To obtain $N_{d,w}$, the number of delta rays per proton from the 0.05-cm-thick window, equation (A1) is integrated over the range of T' and then multiplied by N_e , the number of electrons per cm^2 in aluminum, and by $\rho = 2.72 \text{ g/cm}^3$, the density of aluminum, to give

$$N_{d,w} = \rho N_e \int \frac{d\sigma}{dT'} T' \quad (\text{A3a})$$

$$N_{d,w} = \rho N_e \pi \frac{N_A Z}{A} r_e^2 \frac{2m_e}{\beta^2} \left[\frac{-1}{T'} - \frac{\beta^2 \ln(T')}{T'_{\max}} + \frac{1}{2} \frac{T'}{(T + m_p)^2} \right] \Bigg|_{T' = 0.67 \text{ MeV}}^{T'_{\max} = 1.72 \text{ MeV}} \quad (\text{A3b})$$

$$N_{d,w} = 8.86 \times 10^{-3} \quad (\text{A3c})$$

APPENDIX A

where

$$N_e = N_A \frac{Z}{A} \rho t_w$$

and where the thickness of the entrance window t_w is 0.051 cm.

As stated previously, the lead core of the cup is surrounded by a 0.32-cm-thick copper jacket. The incident protons produce delta rays in this jacket that backscatter into the reentrant portion of the cup. Now the range of 1.72-MeV electrons in copper is given in reference 12 as 1.13 g/cm². If proton-electron collisions are assumed to occur at an average depth of 0.557 g/cm², then only those electrons backscattered with energy greater than 0.9 MeV can escape from the base. To estimate $N_{d,b}$, the number of delta rays which occur in the jacket, the right side of equation (A3b) is evaluated from $T' = 0.9$ MeV to $T'_{\max} = 1.72$ MeV where for copper $Z = 29$, $A = 63.54$, and $\rho = 8.92$ g/cm³; the result is

$$N_{d,b} = 9.24 \times 10^{-2}$$

If the delta rays are scattered isotropically in 4π geometry, then the number of back-scattered delta rays per proton that can escape the cup is given by

$$N_{d,e} = N_{d,b} \frac{1}{2} \left[1 - \cos \left(\tan^{-1} \frac{d}{k} \right) \right] = 8.3 \times 10^{-5}$$

where the inside diameter of the cup d is 15.24 cm and the distance from the base to the near end of the cup extension k is 76.20 cm.

The loss of electrons from the cup would cause an apparent increase from the true proton current, whereas the addition of electrons (delta rays from window) would cause an apparent decrease from the true proton current. From these calculations the number of delta rays $N_{d,w}$ from the window is much larger than the backscattered delta rays $N_{d,e}$ that can escape from the cup; thus the decrease from the true proton current would be approximately

$$\frac{N_{d,w} - N_{d,e}}{100} = 0.88 \text{ percent}$$

APPENDIX B

ERROR PRODUCED BY COMPTON ELECTRONS

In Compton scattering, gamma rays or X-rays undergo elastic collisions with free electrons (assumed to be initially at rest). The kinetic energy T_e of a recoil electron is given by

$$T_e = T_\gamma \left[\frac{2\alpha}{1 + 2\alpha + (1 + \alpha)^2 \tan^2 \phi} \right] \quad (\text{B1})$$

where

T_γ energy of incident photon, MeV

α = T_γ/m_e

m_e rest mass of electron, MeV

ϕ angle of recoil electron to direction of incident photon, deg

The maximum energy of the recoil electron occurs when $\phi = 0$, that is,

$$(T_e)_{\max} = T_\gamma \left(\frac{2\alpha}{1 + 2\alpha} \right) \quad (\text{B2})$$

The average energy per Compton electron is given by

$$(T_e)_{\text{av}} = T_\gamma \frac{e_a^\sigma}{e^\sigma} \quad (\text{B3})$$

where e_a^σ is the average absorption cross section and e^σ is the average collision cross section. On page 688 of reference 13, e_a^σ is given as

$$e_a^\sigma = 2\pi r_e^2 \left[\frac{2(1 + \alpha)^2}{\alpha^2(1 + 2\alpha)} - \frac{1 + 3\alpha}{(1 + 2\alpha)^2} - \frac{(1 + \alpha)(2\alpha^2 - 2\alpha - 1)}{\alpha^2(1 + 2\alpha)^2} \right. \\ \left. - \frac{4\alpha^2}{3(1 + 2\alpha)^3} - \left(\frac{1 + \alpha}{\alpha^3} - \frac{1}{2\alpha} + \frac{1}{2\alpha^3} \right) \ln(1 + 2\alpha) \right] \text{cm}^2/\text{electron} \quad (\text{B4})$$

APPENDIX B

and e^σ is given on page 684 of reference 13 as

$$e^\sigma = 2\pi r_e^2 \left\{ \frac{1 + \alpha}{\alpha^2} \left[\frac{2(1 + \alpha)}{1 + 2\alpha} - \frac{1}{\alpha} \ln(1 + 2\alpha) \right] + \frac{1}{2\alpha} \ln(1 + 2\alpha) - \frac{1 + 3\alpha}{(1 + 2\alpha)^2} \right\} \text{ cm}^2/\text{electron} \quad (\text{B5})$$

where r_e is the classical radius of the electron (r_0 in ref. 13).

To estimate the charge lost by Compton electrons escaping from the outer surface of the cup, the following assumptions were made:

- (1) Each incident proton undergoes an inelastic collision and produces one 3-MeV gamma ray.
- (2) The probability of producing a gamma ray at a given distance in the base is a function of the inelastic proton-nucleus cross section.
- (3) The gamma rays are emitted isotropically from the point of inelastic collision.
- (4) The probability that a 3-MeV gamma ray will reach the copper jacket on the cup is given by $\exp(-\mu X)$ where μ is the mass attenuation coefficient and X is the distance in g/cm^2 of lead from the point of production to the surface.

The average energy per Compton electron produced by 3-MeV gamma rays is 1.73 MeV as calculated from equation (B3). Electrons of this energy have a range in copper of approximately $1.16 \text{ g}/\text{cm}^2$, and since the thickness of the copper jacket is $2.832 \text{ g}/\text{cm}^2$, only those electrons produced near the surface will, on the average, escape. Of course, the energy distribution of Compton electrons varies from a maximum energy of 2.76 MeV (calculated from eq. (B2)) to a zero minimum energy; therefore, the shape of the energy distribution and the location of Compton electron production determine the number of escape particles. The differential cross section for giving an electron a recoil energy between T and $T + dT$ is given (in notation of present paper) by equation (41) on page 54 of reference 14 as

$$\frac{d_e \sigma}{dT} = \frac{\pi r_e^2}{\alpha^2 m_e} \left\{ 2 + \left(\frac{T}{T_\gamma - T} \right)^2 \left[\frac{1}{\alpha^2} + \frac{T_\gamma - T}{T_\gamma} - \frac{2(T_\gamma - T)}{\alpha T} \right] \right\} \quad (\text{B6})$$

APPENDIX B

and the number of Compton electrons produced with energy between $(T_e)_{\max}$ and 0 in an element of thickness Δx_i in the jacket is given by

$$\left. \begin{aligned}
 (N_e^c)_i &= N_A \frac{Z}{A} \rho \Delta x_i \int_0^{(T_e)_{\max}} \frac{d_e \sigma}{dT} dT \\
 (N_e^c)_i &= N_A \frac{Z}{A} \rho \Delta x_i \frac{\pi r_e^2}{\alpha^2 m_e} \left\{ T \left(\frac{\alpha^2 + 4\alpha + 1}{2\alpha^2} \right) + \frac{1}{\alpha^2} \left[-3T_\gamma^2 - T_\gamma \ln (T_\gamma - T)^2 \right] \right. \\
 &\quad \left. - \frac{1}{2T_\gamma} (T_\gamma - T)^2 + 2(T_\gamma - T) - T_\gamma \ln [T_\gamma (T_\gamma - T)] \right. \\
 &\quad \left. + \frac{2}{\alpha} \left[T + T_\gamma \ln (T_\gamma - T) \right] \right\} \Bigg|_0^{(T_e)_{\max}}
 \end{aligned} \right\} \quad (B7)$$

where

- N_A Avogadro's number, 6.0225×10^{23} atoms/mol
- Z atomic charge of element, 29 for copper
- A mass number of element, 63.54 for copper
- ρ density of element, 8.96 g/cm³ for copper

The number $(N_e^c)_i$ of electrons that can escape the jacket is a function of the depth x in the jacket at which they are produced. At a given depth there is a minimum electron energy $(T_e(x_i))_{\min}$ below which the electrons cannot escape. Thus, the number of Compton electrons N_e^c escaping from the surface for each 3-MeV gamma ray interacting within the copper jacket can be estimated by the following expression:

$$N_e^c = \sum_i (N_e^c)_i \int_{(T_e(x_i))_{\min}}^{(T_e)_{\max}} \frac{d_e \sigma}{dT} dT \quad (B8)$$

APPENDIX B

where

$$\sum_i x_i = 2.832 \text{ g/cm}^2$$

If N_p incident protons each produce one 3-MeV gamma ray and if the probability of a 3-MeV gamma ray reaching the copper jacket is $\exp(-\mu X)$, then the total number N_e of Compton electrons leaving the surface for N_p incident protons is given by

$$N_e = N_e^c \sum_{j=1}^{N_p} \exp(-\mu X_j) \quad (B9)$$

To evaluate this equation, a computer program was written which used the Monte Carlo technique. The base of the cup (345.6 g/cm² thick) was divided into 300 segments, each 1 g/cm² thick, to approximate the range of 600-MeV protons in lead, 300.7 g/cm². A beam of 600-MeV protons, assumed to be parallel, is incident on the cup along the cup center line. Each proton is multiply scattered through intervening segments until it comes to a randomly selected slab. At the selected segment the lateral displacement of the proton from its incident trajectory is calculated. Next, a random direction is selected, the straight-line thickness X to the surface is calculated, and the coordinates of the point of intersection with the surface are determined. The probability that a proton-nucleus interaction will occur after traversing a distance ℓ in lead from the point of entry to the selected segment is given by

$$P_{\text{inelastic}} = 1 - \exp\left(-N_A \int_0^{\ell} \frac{\sigma}{A} dx\right)$$

where σ is the inelastic proton-nucleus cross section. The probability value is used to form a weighted distribution of gamma rays produced in the cup.

As an aid in plotting the intensity distribution of electrons leaving the surface, the cylindrical surface was divided into 100 bands, each 1.016 cm wide, and the base end was divided into 10 concentric rings, each 1.016 cm wide. The coordinates of each electron leaving the surface were tested to determine which band was used to catalog the particle. Note that the cylindrical bands have equal areas, $A_{\text{cyl}} = \pi R_{\text{cyl}}^2 w = 329.48 \text{ cm}^2$, but the concentric rings on the base have unequal areas given by

$$A_b = \pi \left[(n+1)^2 - n^2 \right] w^2 \quad (n = 0, 1, 2, \dots, 9)$$

where w is the width of the bands and R_{cyl} is the radius of the cylinder.

APPENDIX B

For a total of N_p incident protons, the number N_e of electrons leaving the surface was obtained from the program by evaluating equation (B9). However, in figure 5 the number of electrons leaving the surface in each band is plotted as a function of distance (band number) along the surface. The four curves shown in the figure correspond to incident beam radii of 0, 2, 4, and 6 cm. Each curve is based on 11 000 incident proton histories in the computer program. The percent charge loss from the cup by Compton electrons is given in table II.

APPENDIX C

IONIZATION OF RESIDUAL GAS

To estimate the number of ions pairs formed per incident 600-MeV proton, the residual gas is assumed to be principally nitrogen at a pressure of 5×10^{-5} torr (1 torr = 133 Pa). The residual gas occupies a volume whose length l from the entrance window to the cup is 114.83 cm. The number of ion pairs per proton is given by

$$\frac{\text{Ion pair}}{\text{Proton}} = \frac{(dE/dx)l\rho R}{W}$$

where

dE/dx rate of energy loss per unit path length in nitrogen, $2.265 \frac{\text{MeV-cm}^2}{\text{g}}$ (ref. 8)

ρ density of nitrogen under standard conditions, 1.2504 mg/cm^3

W energy required to produce one ion pair in nitrogen, 36.3 eV (ref. 10)

R ratio of chamber pressure to standard atmospheric pressure, $\frac{5 \times 10^{-5} \text{ torr}}{7.60 \times 10^2 \text{ torr}}$

Evaluating this expression shows that

$$\frac{\text{Ion pairs}}{\text{Proton}} = 5.9 \times 10^{-4}$$

which is negligibly small compared with other possible errors.

APPENDIX D

CHARGE LOST THROUGH PROTON-NUCLEUS COLLISIONS

The probability of a proton-nucleus collision is quite large for a 600-MeV incident proton coming to rest in lead. It is assumed that the probability of inelastic collisions is given by the expression

$$P_{\text{inelastic}} = 1 - \exp\left(-N_A \int_0^{\ell} \frac{\sigma}{A} dx\right)$$

or, by changing the variable of integration from path length to energy,

$$P_{\text{inelastic}} = 1 - \exp\left(-N_A \int_0^{E_I} \frac{\sigma}{A} \frac{dE}{\frac{1}{\rho} \frac{dE}{dx}}\right) \quad (\text{D1})$$

where

σ	total inelastic cross section, cm^2
A	mass number, g/mol
ℓ	particle path length in absorber, g/cm^2
N_A	Avogadro's number, atoms/mol
ρ	density of absorber, g/cm^3
dE/dx	rate of energy loss per unit path length in absorber
E_I	incident kinetic energy

Evaluating equation (D1) for 600-MeV protons stopping in lead shows that, on the average, approximately 0.758 percent of the incident particles undergo an inelastic collision.

If the energy of nucleons within the nucleus is ignored and it is assumed that an incident proton interacts with individual nucleons or small clusters (deuterons, tritons, helium nuclei, etc.), then from relativistic kinematics, the maximum energy of the most prevalent charged secondaries is given by

APPENDIX D

$$T = \frac{2m_t \cos^2 \theta}{\frac{1}{\bar{\beta}^2} - \cos^2 \theta} \quad (D2)$$

For $\theta = 0$,

$$T = \frac{2m_t}{\frac{1}{\bar{\beta}^2} - 1}$$

and

$$T = \frac{2m_t p_I^2}{(E_I \pm m_t)^2 - p_I^2} \quad (D3)$$

where

$$\bar{\beta}^2 = \frac{p_I}{(E_I \pm m_t)^2}$$

p_I momentum of incident particle, MeV/c

T_I kinetic energy on incident particle, MeV

T kinetic energy of recoil particle, MeV

E_I total energy of incident particle, $T_I^2 + m_I^2$, MeV

m_I rest mass of incident particle, MeV

m_t rest mass of target particle, MeV

θ angle of recoil relative to incident particle direction, deg

Equation (D3) was evaluated and the range in lead of the five most prevalent secondaries was calculated by using equation 14 of reference 15. This range was compared with the cup base thickness. Table V gives the results of these calculations. Since the thickness of the cup base is 345.6 g/cm², the loss of charge through the cup end by recoil particles is remote.

APPENDIX D

The charge lost from the cup by neutron-proton collisions near the surface was considered to be the most probable mechanism for the emission of protons from the surface. For each proton-nucleus interaction in lead there are a large number of neutrons emitted. In figure 6 the average number of neutrons per interaction in lead is plotted as a function of incident proton energy. The data points were obtained from calculations given in reference 16. Most of the neutrons from the inelastic events are produced through nuclear deexcitation with energies generally less than 5 MeV. The cascade neutrons can have energies up to the energy of the incident proton and they can undergo a neutron-nucleus interaction with the emission of a proton which may have sufficient energy to leave the cup.

To estimate the number of protons lost from the cup, the following method was employed in a Monte Carlo computer program. Since the range of 600-MeV protons in lead is 300.7 g/cm^2 , the cup base was divided into 300 slabs, each 1 g/cm^2 thick; it was assumed that each incident proton lost kinetic energy ΔT_i in the i th slab and was deflected through an average angle $\langle \theta \rangle_i$ by multiple scatterings. The probability P that a proton-nucleus interaction will occur in the i th slab is given by

$$P = 1 - \exp\left(-N_A \int_{T_{\text{in}}}^{T_{\text{out}}} \frac{\sigma}{A} \frac{dT}{\frac{1}{\rho} \frac{dT}{dx}}\right) \quad (\text{D4})$$

where T_{in} and T_{out} are the kinetic energy of the proton entering the slab and the kinetic energy of the outgoing particle, respectively; $\Delta T_i = T_{\text{in}} - T_{\text{out}}$.

To simplify the computational details, it is assumed that each proton-nucleus collision can be replaced by an elastic collision between the incident proton and a neutron or cluster of neutrons. The momentum p'_p of the scattered proton and the momentum p'_n of the recoil neutron or cluster of neutrons are calculated from the following relativistic two-body kinematical equations:

$$p'_p = \frac{\bar{\beta} E_p c \cos \theta_p \pm \left[(E_p c)^2 - \bar{\gamma}^2 m_p^2 (1 - \bar{\beta}^2 \cos^2 \theta_p) \right]^{1/2}}{\bar{\gamma} (1 - \bar{\beta}^2 \cos^2 \theta_p)} \quad (\text{D5})$$

$$p'_n = \left[(p'_p)^2 \sin^2 \theta_p + (\bar{\beta} \bar{E} - E'_p \cos \theta_p)^2 \right]^{1/2} \quad (\text{D6})$$

APPENDIX D

and

$$\tan \theta_n = \frac{\sin \theta_p}{\cos \theta_p - \frac{\bar{\beta} E}{p'_p}} \quad (D7)$$

where

- m_p rest mass of incident proton
- m_n mass of neutron or neutron cluster
- p_p momentum of incident proton
- E_p total energy of incident proton
- E'_p total energy of scattered proton
- θ_p angle of scatter of proton
- θ_n angle of recoil of neutron or neutron cluster

and

$$\bar{E} = E_p + m_n$$

$$\bar{\beta} = \frac{p_p}{E_p + m_n}$$

$$\bar{\gamma} = \frac{1}{1 - \bar{\beta}^2}$$

$$E_p^c = \frac{E^c}{2} \left[1 + \frac{m_p^2 - m_n^2}{(E^c)^2} \right]$$

$$E^c = \left[(m_p + m_n)^2 + 2T'_p m_n \right]^{1/2}$$

APPENDIX D

The kinetic energy T'_p of the scattered proton is given by

$$T'_p = \left[m_p^2 + (p'_p)^2 \right]^{1/2} - m_p$$

and the kinetic energy of the recoil neutron or cluster by

$$T'_n = \left[m_n^2 + (p'_n)^2 \right]^{1/2} - m_n$$

A computer program, which incorporated equations (D4) to (D7), was written to simulate the energy loss and scattering of the incident protons, proton-neutron elastic collisions, and subsequent neutron-proton scattering. It is assumed that the incident beam of protons has a uniform density distribution and has no divergence. Each proton is multiply scattered through intervening slabs to a randomly selected i th slab. An angle of scatter for the proton in the i th slab is randomly selected over the interval $0 < \theta_p \leq \pi/2$. Equations (D5) to (D7) are evaluated by using θ_p and the total energy E_p of the proton in the i th slab to obtain the scattered proton energy E'_p and energy of the recoil neutron E'_n . Equation (D4) is evaluated to give the probability of an inelastic event. The distance from the point of collision to the surface is calculated from the scattered proton direction. If the range of the scattered proton of energy E'_p is greater than the distance to the surface, the proton is assumed to have escaped. For a total of N_p incident protons, the number escaping through this mechanism is denoted by N'_p .

To account for the multiple production of neutrons, the data in figure 6 for cascade neutrons was used, as follows: for protons in the energy range from 600 MeV to 400 MeV, assume three cascade neutrons per interaction; from 400 MeV to 50 MeV, assume two neutrons per interaction; and below 50 MeV, assume one neutron per interaction. The available recoil energy from the elastic scattering of a cluster of two or three neutrons is divided among the particles at random. It is further assumed that the recoil neutrons travel parallel to the direction defined by θ_n . Each neutron of the initial cluster has a probability P'' of having a collision with a nucleus at a randomly chosen point along its trajectory. The probability P'' of such an event is given by

$$P'' = 1 - \exp\left(-N_A \int \frac{\sigma}{A} dx\right) \quad (D8)$$

where the cross section σ is understood to be for a neutron-nucleus collision in lead. The inelastic proton-nucleus and neutron-nucleus cross sections are nearly the same as

APPENDIX D

the cross sections shown in figure 4 of reference 17. For each neutron-nucleus event, the distance to the surface along the incident neutron direction is compared with the range of the tertiary proton. If the range is greater than the distance, the proton escapes from the cup. The number of protons escaping through neutron-proton interactions is denoted by N_p'' . The total number of protons escaping from the cup for N_p incident protons is the sum of N_p' and N_p'' .

The foregoing procedure indicated that an extremely small number of protons were lost from the cup. The program was rerun with the requirement that each secondary neutron have a knock-on collision with a proton, that is, $P'' = 1$. This overestimate is used as the percent charge loss shown in table III.

The foregoing discussion has assumed a parallel incident beam. No calculations have been made for a divergent beam. However, if the incident beam is focused to a point on the front face of the base and the beam is entirely within the diameter of the cup extension, then the angle of divergence is approximately 3° . If the focus point is moved along the center line toward the entrance window, no charge is lost because of penetration by the incident beam until a point approximately 50.8 cm from the entrance window is reached (divergence of 7.1°). At this point some of the incident protons will pass through the sides of the cup.

REFERENCES

1. Crandall, Walter E.; Millburn, George P.; Pyle, Robert V.; and Birnbaum, Wallace: $C^{12}(x,xn)C^{11}$ and $Al^{27}(x,x2pn)N_a^{24}$ Cross Sections at High Energies. Phys. Rev., second ser., vol. 101, no. 1, Jan. 1, 1956, pp. 329-337.
2. Aamodt, R. Lee; Peterson, Vincent; and Phillips, Robert: $C^{12}(p,pn)C^{11}$ Cross Section From Threshold to 340 Mev. Phys. Rev., second ser., vol. 88, no. 4, Nov. 15, 1952, pp. 739-744.
3. Hicks, H. G.; Stevenson, P. C.; and Nervik, W. E.: Reaction $Al^{27}(p,3pn)N_a^{24}$. Phys. Rev., second ser., vol. 102, no. 5, June 1, 1956, pp. 1390-1392.
4. Parilkh, Vastupal: Absolute Cross-Sections of $C^{12}(p, pn)C^{11}$ From 288 to 383 MeV. Nucl. Phys., vol. 18, no. 4, Sept. 1960, pp. 628-637.
5. Chamberlain, O.; Segrè, E.; and Wiegand, C.: Experiments on Proton-Proton Scattering From 120 to 345 Mev. Phys. Rev., second ser., vol. 83, no. 5, Sept. 1, 1951, pp. 923-932.
6. Brown, K. L.; and Tautfest, G. W.: Faraday-Cup Monitors for High-Energy Electron Beams. Rev. Sci. Instrum., vol. 27, no. 9, Sept. 1956, pp. 696-702.
7. Santoro, R. T.; and Peelle, R. W.: Measurement of the Intensity of the Proton Beam of the Harvard University Synchrocyclotron for Energy-Spectral Measurements of Nuclear Secondaries. ORNL-3505, U.S. At. Energy Comm., Mar. 1964.
8. Janni, Joseph F.: Calculations of Energy Loss, Range, Pathlength, Straggling, Multiple Scattering, and the Probability of Inelastic Nuclear Collisions for 0.1- to 1000-Mev Protons, AFWL-TR-65-150, U.S. Air Force, Sept. 1966. (Available from DDC as AD 643 837.)
9. Bakker, C. J.; and Segrè, E.: Stopping Power and Energy Loss for Ion Pair Production for 340-MeV Protons. Phys. Rev., second ser., vol. 81, no. 4, Feb. 15, 1951, pp. 489-492.
10. Staub, Hans H.: Detection Methods. Experimental Nuclear Physics, Volume I, E. Segrè, ed., John Wiley & Sons, Inc., c.1953, pp. 1-165.
11. Rossi, Bruno: High-Energy Particles. Prentice-Hall, Inc., c.1952.
12. Berger, Martin J.; and Seltzer, Stephen M.: Tables of Energy Losses and Ranges of Electrons and Positrons. NASA SP-3012, 1964.
13. Evans, Robley D.: The Atomic Nucleus. McGraw-Hill Book Co., Inc., c.1955.

14. Davisson, C. M.: *Interaction of γ -Radiation With Matter. Alpha-, Beta-, and Gamma-Ray Spectroscopy, Volume I*, Kai Siegbahn, ed., North-Holland Pub. Co. (Amsterdam), 1965, pp. 37-78.
15. Barkas, Walter H.; and Berger, Martin J.: *Tables of Energy Losses and Ranges of Heavy Charged Particles. NASA SP-3013*, 1964.
16. Bertini, Hugo W.: *Nonelastic Interactions of Nucleons and π Mesons With Complex Nuclei at Energies Below 3 GeV.* Phys. Rev. C, third ser., vol. 6, no. 2, Aug. 1972, pp. 631-659.
17. Barashenkov, V. S.; Gudima, K. K.; and Toneev, V. D.: *Cross Sections for Fast Particles and Atomic Nuclei.* Progr. Phys., vol. 17, no. 10, 1969, pp. 683-725.

TABLE I.- ESTIMATED WEIGHT OF FARADAY CUP

Component	Weight, kg
Cup	235.9
Vacuum housing	131.5
Carriage	81.6
Vacuum diffusion pump	49.9
Magnet	81.6
Power supply for magnet	36.3
Total weight	616.9

TABLE II.- PERCENT CHARGE LOSS THROUGH COMPTON EFFECT
FOR SEVERAL INCIDENT PROTON BEAM RADII

Beam radius, cm	Charge loss, percent incident charge
0	0.073
2	.061
4	.057
6	.063

TABLE III.- CHARGE LOSS DUE TO PROTON LEAKAGE FROM CUP BASE

[Incident beam assumed nondivergent]

Beam diameter, cm	Charge loss, percent incident charge
0	0.009
4	.010
8	.014
12	.020

TABLE IV.- SUMMARY OF ESTIMATED ERRORS

Source of error	Charge loss, percent incident charge
Delta rays	-0.88
Tertiary electrons	(a)
Compton electrons from surface	0.06
Ion formation in residual gas	(a)
Neutron-proton collisions	-0.02
Pi-mesons	(a)
Total decrease from true current	-0.83

^aNegligible.

TABLE V.- MAXIMUM RECOIL ENERGY OF CHARGED SECONDARIES
FROM INCIDENT 600-MeV PROTONS

Secondary particle	Maximum energy, MeV	Range in lead, g/cm ²
Proton	600	300.7
Deuteron	547	178.2
Triton	479	110.9
Helium-3	479	27.64
Helium-4	421	36.7

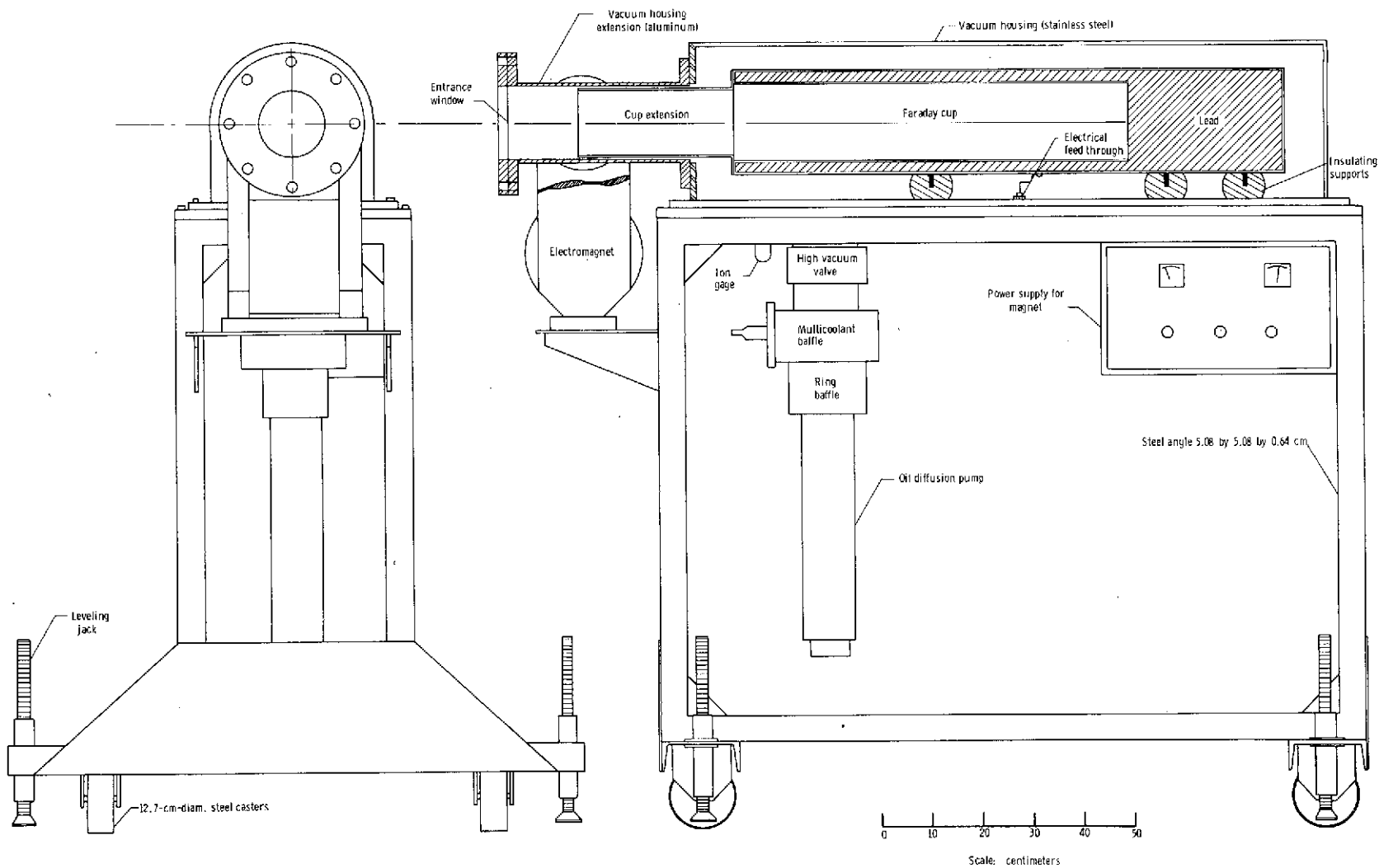


Figure 1.- Schematic drawing of complete Faraday cup assembly.

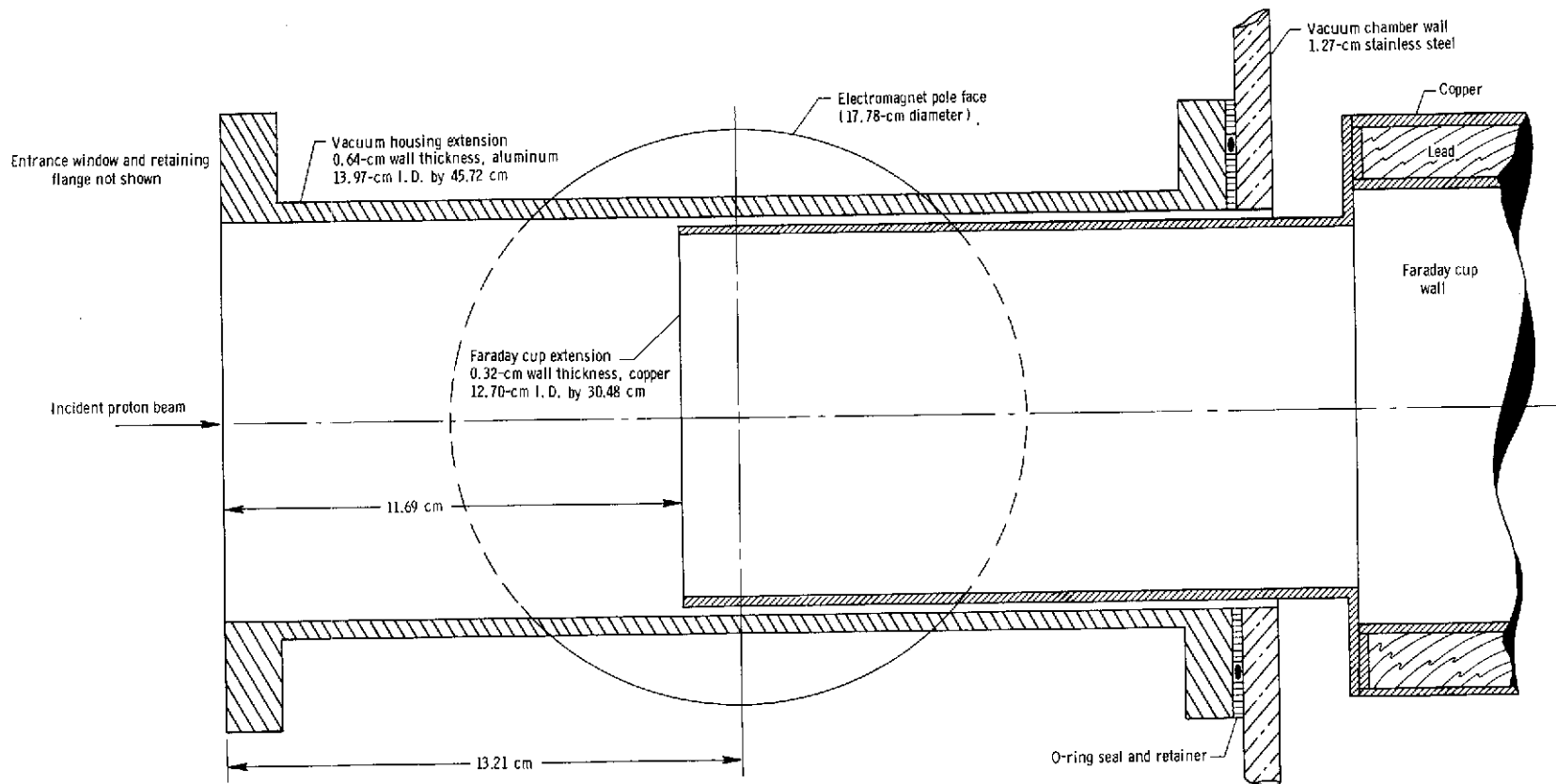


Figure 2.- Faraday cup extension and location of electromagnet pole face.

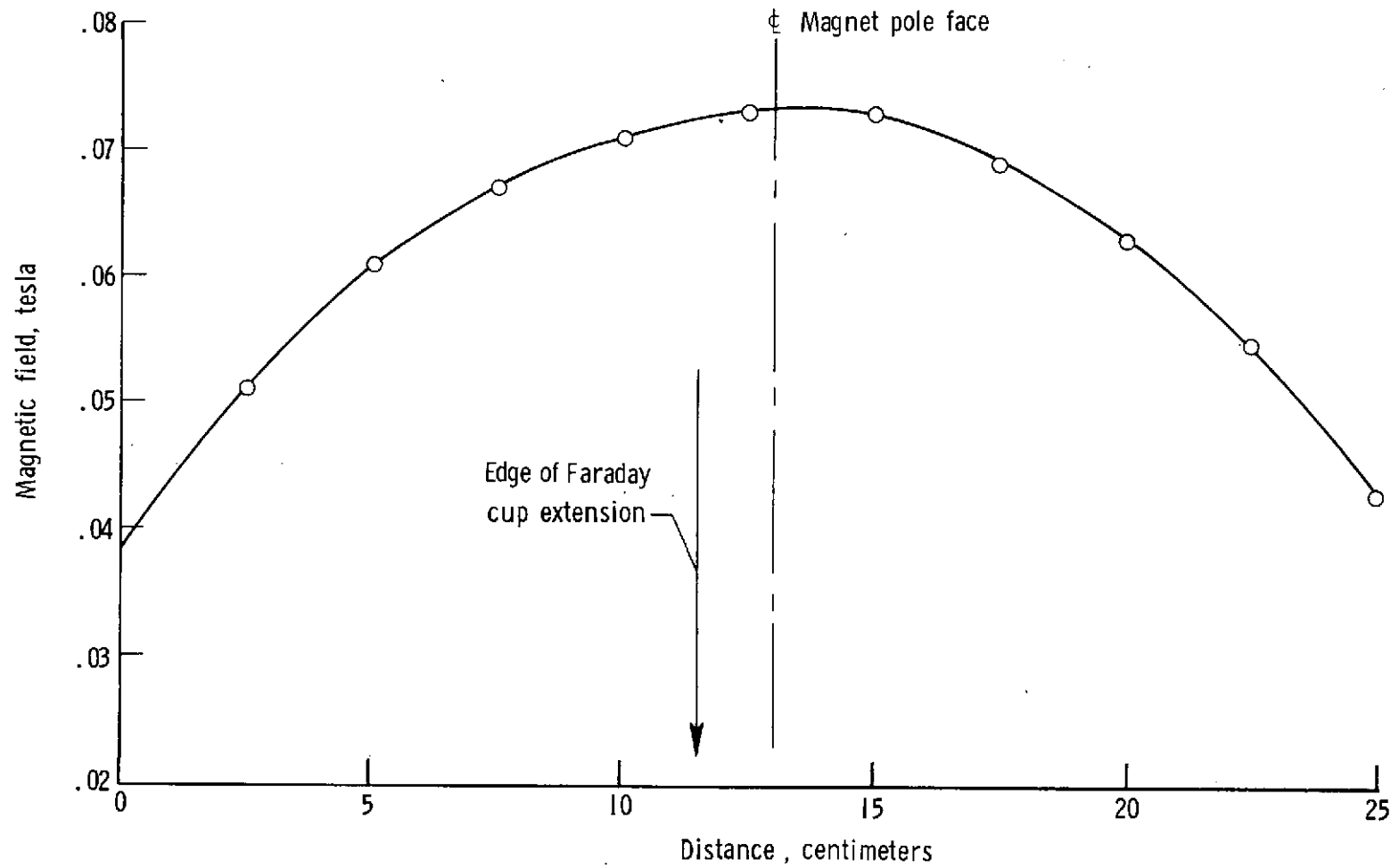


Figure 3.- Magnetic field along center line of Faraday cup from entrance window to a depth of 25.4 cm. 3-A current.

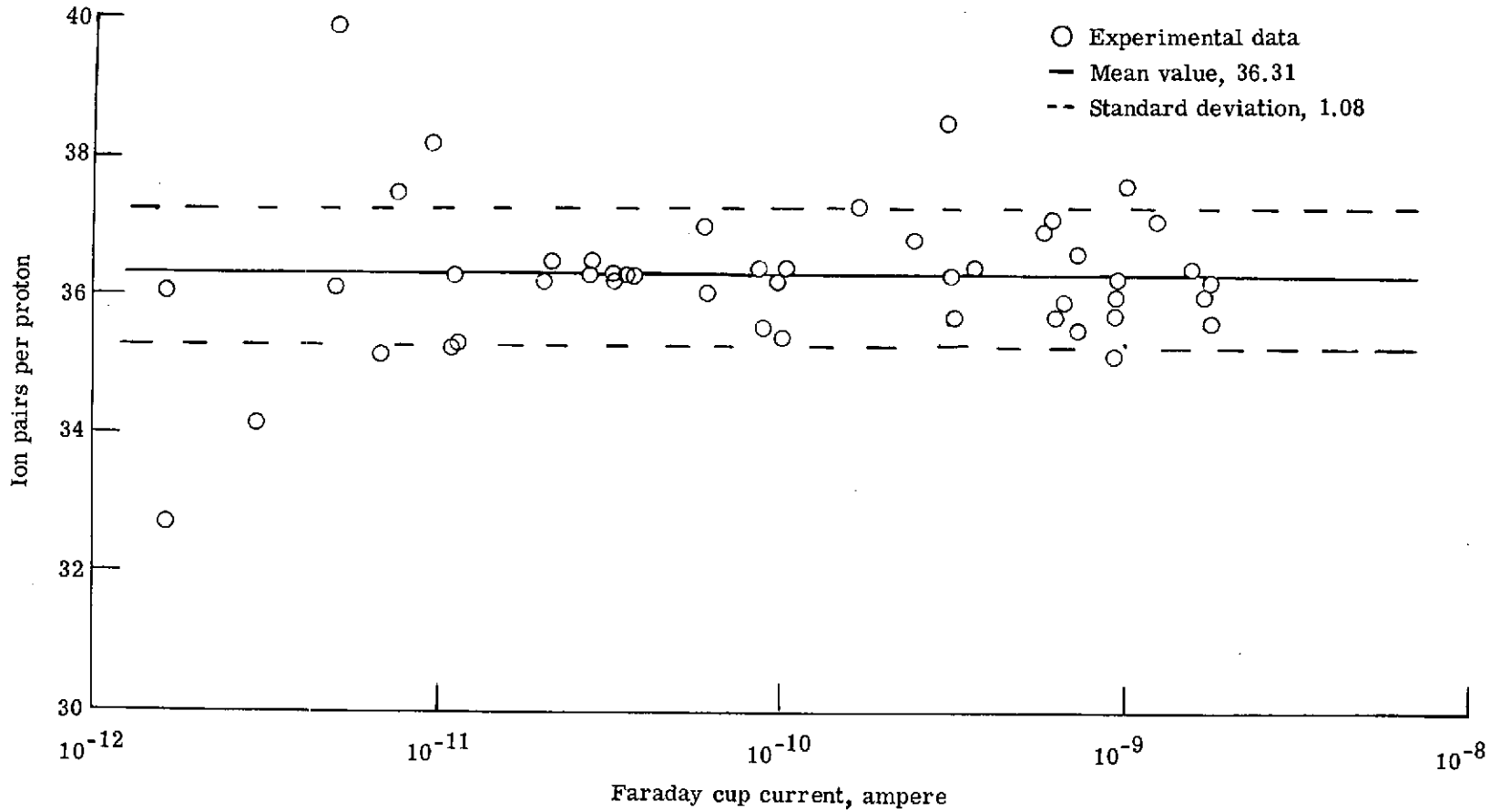


Figure 4.- Calibration data for helium-filled ion chamber.

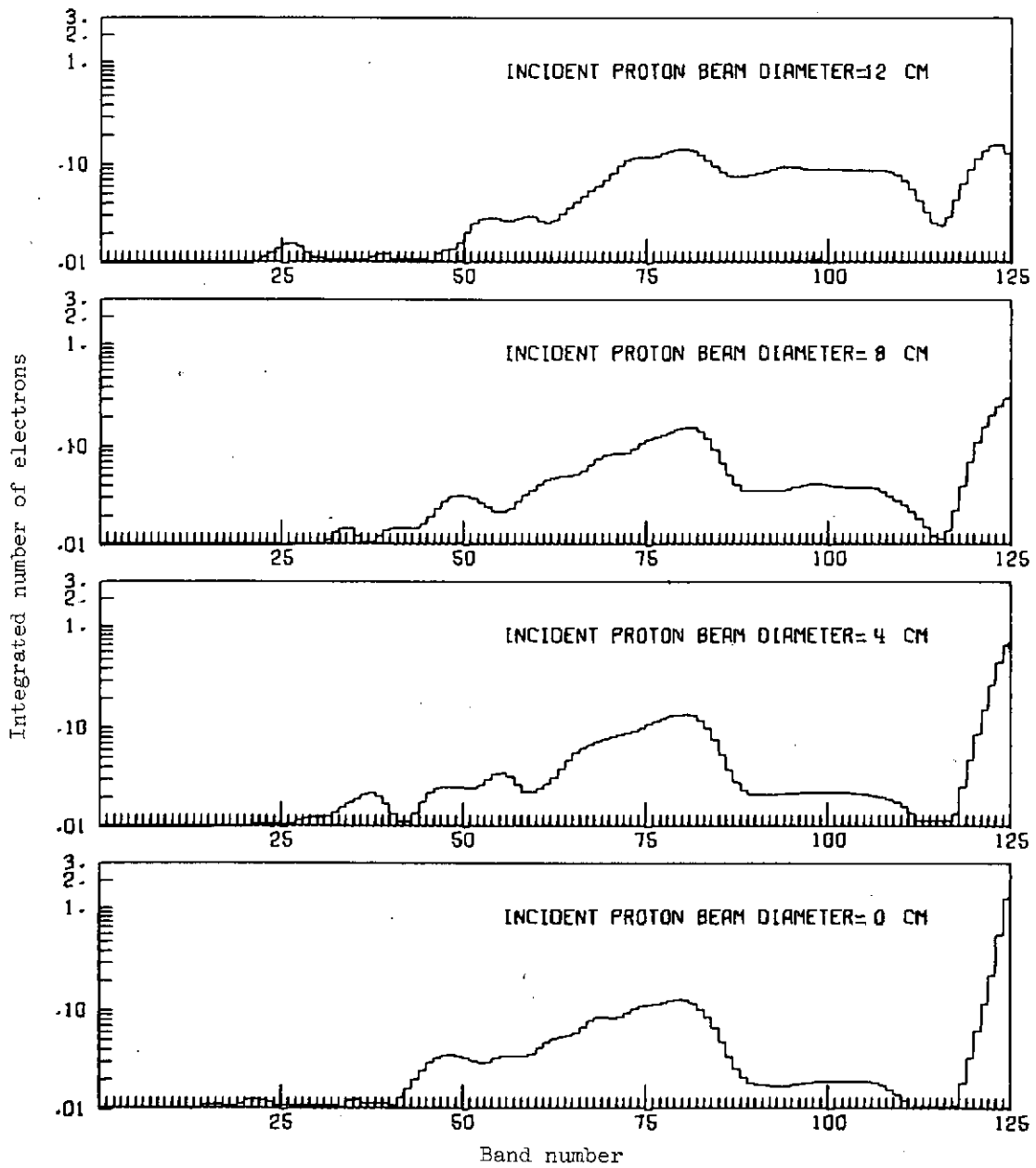


Figure 5.- Monte Carlo calculation of intensity distribution of electrons escaping from surface of Faraday cup.

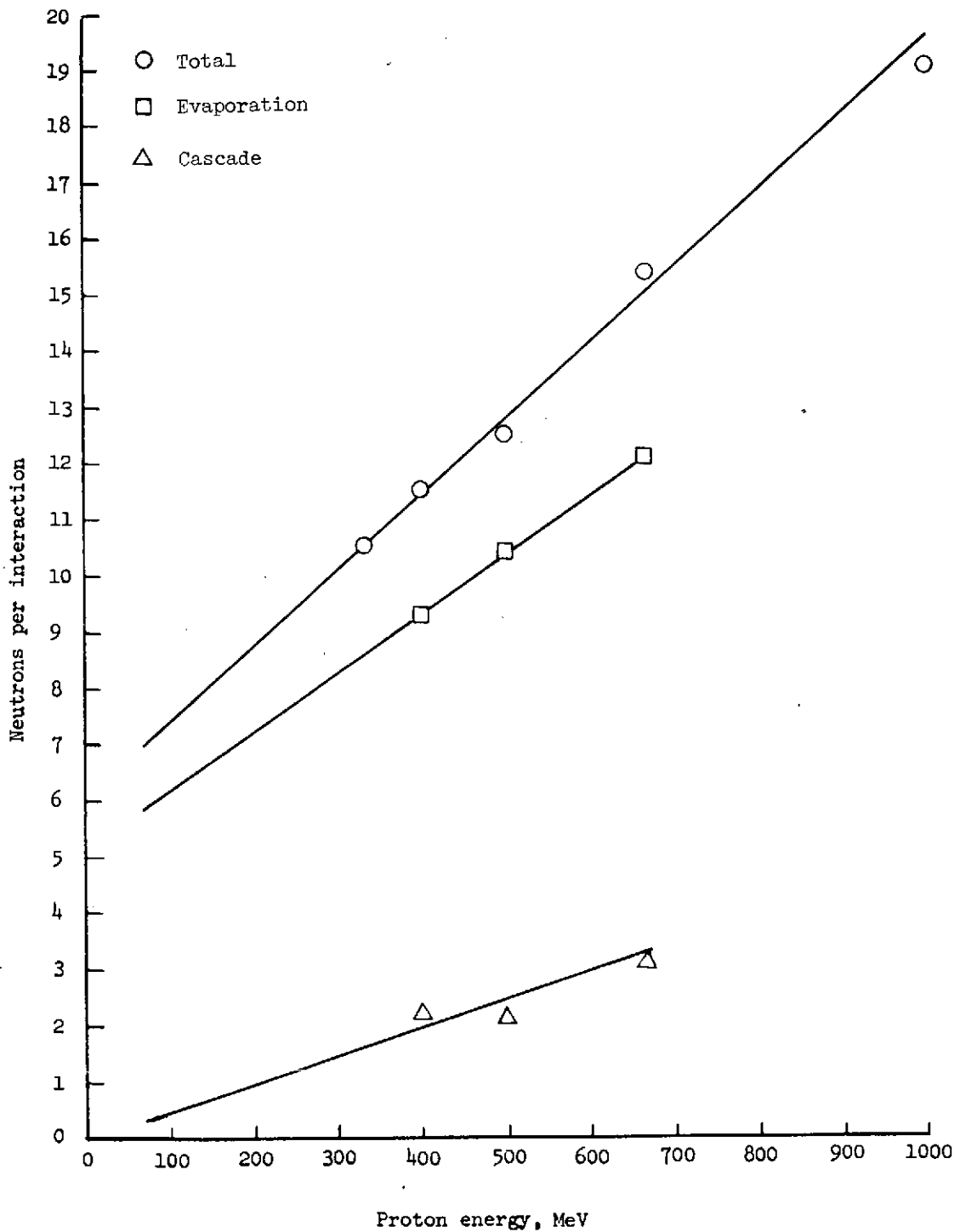


Figure 6.- Neutrons produced per proton-nucleus interaction in lead. Data points were obtained from calculations given in reference 16. Solid lines are used only to indicate trend.